Development and use of a Velocity Prediction Program to compare the effects of changes to foil arrangement on a hydro-foiling Moth dinghy

M W Findlay, **S R Turnock**, School of Engineering Sciences, University of Southampton, UK

SUMMARY

The International Moth dinghy is a 3.355m long single handed, una-rigged monohull dinghy. The class rules allow the use of hydrofoil that in certain wind conditions can significantly reduce resistance. A new velocity prediction program (VPP) has been developed to evaluate the impact of hydrofoil design and set-up on the performance of a Moth dinghy by simulating racing on a windward - leeward course. The VPP generates polar diagrams indicating the speed of the craft in a range of true wind strengths and angles. Sail force and windage are modelled using aerofoil theory. The drag model includes hull skin friction and residuary resistance, profile and induced drag for every foil, wavemaking drag of the lifting foils and spray drag of the surface piercing foils. Using an iterative process the VPP determines the boat speed that balances resistive forces with drive force, heeling moment and righting moment and vertical lift forces with weight. A series of case studies demonstrate the use of the VPP by examining the effects of changing the span of the forward foil, adding end plates, and using different foil geometries on performance.

NOMENCLATURE

$(1+k)$	Form factor	[-]
A_G	Geometric Aspect ratio	[-]
AR_g	Geometric Aspect ratio	[-]
β_a	Apparent wind angle	[deg]
b	Breadth of sail	[m]
c	Chord of foil	[m]
C_D	Coefficient of drag	[-]
C_{D_i}	Coefficient of induced drag	[-]
C_{D_f}	Coefficient of skin friction	[-]
C_{D_p}	Coefficient of profile drag	[-]
C_{D_r}	Drag coefficient of rth component	[-]
C_{Dspray}	Coefficient of spray drag	[-]
C_L	Coefficient of lift	[-]
C_{L1}	Coefficient of lift on foil 1	[-]
C_{L2}	Coefficient of lift on foil 2	[-]
C_W	Coefficient of wavemaking drag	[-]
D	Drag	[N]
D_{Spray}	Spray drag	[N]
D_W	Drag due to windage	[N]
Δ_e	Effective hull displacement	[N]
f_x	Side force (body axis system)	[N]
f_y	Drive force (body axis system)	[N]
g	Acceleration due to gravity; 9.81	[m/s^2]
h	Depth of submergence	[m]
κ_1	Constant for end plates efficiency	[-]
κ_2	Constant for taper ratio	[-]
k	Induced drag slope	[-]
k_0	Wavenumber	[m^{-1}]
L	Length scale (in context of R_N)	[m]
L	Sail lift	[N]
L_1	Lift from forward foil	[N]
L_2	Lift from aft foil	[N]
M	Heeling moment	[Nm]
m_{crew}	Mass of helmsperson	[kg]
ρ_{air}	Density of air	[kg/m^3]
ρ	Density of water	[kg/m^3]
R_N	Reynolds number	[-]
RM_{Max}	Maximum righting moment	[Nm]
S	Area of foil	[m^2]
S_r	Area of rth component	[m^2]
S_{sail}	Sail area	[m^2]
t	Thickness of foil	[m]
U	Velocity scale	[m/s]
ν	Kinematic viscosity	[m^2/s]
v_a	Apparent wind speed	[m/s]
v_S	Craft speed through water	[m/s]
v_T	True wind speed	[knots]
W	Total weight of craft and crew	[N]
x	Lever arm of righting moment	[m]
x_1	Hor. dist. CG to CE of foil 1	[m]
x_2	Hor. dist. CG to CE of foil 2	[m]
z	Lever arm of heeling moment	[m]
$z*$	Vert. dist. CE f_y to CE R_{Tot}	[m]

1 INTRODUCTION

Hydrofoils have traditionally been fitted to power craft to reduce drag and therefore power requirements at a given operating speed. The application of hydrofoils to sailing craft has been more problematic for two main reasons.

Firstly, the power to weight ratio of most sailing boats is relatively small because sailing craft need to carry ballast

in order to provide righting moment against the heeling moment from the sails. This limits the application of hydrofoils to catamarans and dinghies which can extend the crew weight on racks or trapezes to provide the necessary righting moment.

Secondly, the operating speed of sailing craft is highly variable, being a function of apparent wind speed and direction, and so the use of hydrofoils is also largely a problem of developing suitable control systems to account for these fluctuations. Most yachts racing classes prohibit surface piercing hydrofoils with the consequence that the effective use of hydrofoils relies on the implementation of mechanical control systems to control fully submerged hydrofoils.

Traditionally the motivation behind retro-fitting hydrofoils to sailing craft has been to increase maximum speed for time trial events such as Weymouth speed week. Developments in this area have been ongoing since the launch of Gordon Baker's 'Monitor' in the 1950s and Don Nigg's 'Flying Fish' in the 1960s. [1]

Chapman [2] developed a number of hydrofoiling sailing craft that were used to make performance measurements, along with foil and strut loadings. The measured force data was used in combination with wind tunnel test data to write velocity prediction programs for two hydrofoiling catamarans when in fully foil-borne mode only. The VPP was subsequently used to make design decisions pertaining to the size of the hydrofoils fitted to the craft to increase average speed around a course.

Recently, with the development of hydrofoils for the International Moth class of dinghy, it been demonstrated that hydrofoils provide a performance gain in a large enough range of conditions that 'foilers' would now be expected to outperform 'non foilers' over a series of races. In 2005 foilers won both the World and European championships.

The International Moth dinghy is a 3.355m long single handed, una-rigged monohull dinghy. The class rules do not limit hull shape, materials or weight, but limitations are placed on length, beam and sail area. As a result the craft have evolved to have extremely narrow waterlines (~0.3m), to be extremely lightweight (<30kg fully rigged) and to have large wings from which the helm hikes. This gives them very good power to weight ratios and makes the class a great platform for the use and development of hydrofoils.

Due to limitations imposed by the class rules these craft use a bi-foil airplane configuration utilising daggerboard and rudder mounted, fully submerged T-foils. An active control mechanism is required to maintain a consistent ride height over a range of speeds which is achieved through the use of a bow-mounted wand sensor controlling a trailing edge flap on the forward (daggerboard-mounted) foil. It is possible to adjust the aft (rudder-mounted) foil manually by either altering the angle of attack or the position of another trailing edge flap, depending on the system. Figure 1 shows an example of a hydrofoiling Moth dinghy.

Figure 1 Hydrofoiling Moth dinghy. [3]

In general the foil design and configuration is selected by the designer based on experience and an empirical understanding of the general effects of parameter changes on performance such as take-off speed and maximum speed. However, as the goal is to deliver performance gains in a range of conditions it is important to also consider the effects of different foil designs under sub-optimal operating conditions, such as in non- and partial foil-borne regimes.

In this paper a computational velocity prediction program (VPP) for hydro-foiling sailboats is developed and used to predict the performance of hydro-foiling Moth dinghies. Input parameters for the VPP are the physical dimensions of the foils, hull and sail, and the output is a series of polar plots that describe the speed of the craft for each true wind angle and strength.

The VPP incorporates both displacement and hydrofoiling modes and uses standard models for all major drag components sail-force. The magnitude of each component of drag may be inspected at any given point which helps the designer to understand why one configuration performs better than another. The polar data may be analysed in the context of a race around a course to determine how different configurations perform in different wind conditions.

2 MODELLING APPROACH AND ASSUMPTIONS

2.1 Overview of Velocity Prediction Program

The VPP determines the boat speed for a given true wind angle and speed using the iterative process shown in Figure 2 and described below.

The apparent wind direction and speed are determined from the boat speed and true wind direction and speed, and then the lift and drag forces due to the sail and structural windage are calculated. These forces are resolved into drive force and side force and the drive force is then maximised under the constraint that the heeling moment may not exceed the maximum available righting moment.

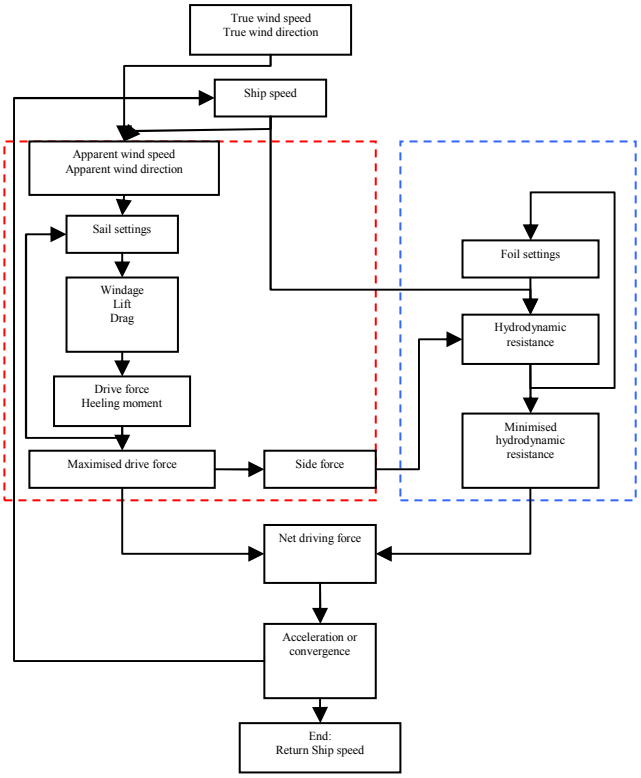

Figure 2 Flow Chart of VPP

The hydrodynamic force model calculates the drag forces due to the hull and foils under the condition that the craft adopts a leeway angle such that the foils provide sufficient lift to counter the sailing side force.

The total hydrodynamic drag varies depending on the trim angles of the foils and whether the boat is in a fully foil-borne or non foil-borne mode. The trim tab angles are varied at each time step until the total hydrodynamic drag is minimised.

The craft is accelerated in accordance with the resulting net drive force and this leads to the next iterative step, beginning with the new hull speed. Once successive time steps result in changes to hull speed that are within a convergence limit the ship speed is deemed to have converged for that true wind condition.

The following sections describe how each force component is modelled in the VPP.

2.2 Windage

Windage is the drag due to zero-lift components such as hull, wings, crew and rigging and wing bar tubing. The mast is not included in the calculation of windage because the pressure distribution over the sail modifies the windage due to the mast. In the case of the foiling moth using a pocket luff and camber induced sails, the windage of the mast is neglected and assumed to be accounted for in the sail profile drag.

$$D_W = 0.5\rho_{air} v_a^2 (\sum_r S_r C_{D_r}) \quad \textbf{(1)}$$

The diameter and area of each physical component included in the windage model was estimated from measurements of a Mistress design of foiling Moth. The drag coefficient for each physical component was estimated from Hoerner [4], based on the sectional shape of the component.

2.3 Sail Force Model

The extremely narrow waterline beam of the International Moth implies that virtually no righting moment is derived from the movement of the centre of buoyancy due to heeling; it is all due to the action of the crew hiking. The effect of heel on righting moment is therefore neglected and the maximum righting moment is:

$$RM_{Max} = xm_{crew} g \quad \textbf{(2)}$$

A value of $x=1.425m$ is used for the Moth, based on the distance of the wing edge from the centreline (1.125m) and the effect of hiking moving the centre of effort of the crew outboard by 0.3m. This was determined using a 'hiking bench' supported on a thin metal rod to find the distance outboard of the bench at which the centre of effort acts. For this paper the mass of the crew was assumed to be constant at 70kg.

The drag force on the sail is assumed to be due to skin-friction, pressure form drag and the induced drag. The total effect of skin friction and pressure form drag is known as profile drag and is calculated based on a skin friction coefficient and a form factor. The form factor modifies the skin friction to account for the alteration of the boundary layer due to the pressure distribution across the sail.

The skin friction coefficient for the sail is calculated based on the Reynolds number of the flow and the ITTC '57 skin friction correlation line.

$$R_N = \frac{UL}{\nu} \quad \textbf{(3)}$$

$$C_{D_f} = \frac{0.075}{(Log(R_N) - 2)^2} \quad \textbf{(4)}$$

Profile drag is calculated from skin friction plus a form factor:

$$C_{D_p} = 2C_{D_f}(1+k) \quad \textbf{(5)}$$

A value of 1.05 was chosen for the form factor, *1+k*, on the basis that the sail is thin and relatively efficient as a result of the pocket luff and cam inducers.

Sail C_L is determined by increasing iteratively from zero to C_{Lmax} and calculating the resulting lift, drag, drive force, side fore and heeling moment. The operating lift coefficient, C_L, is the one that maximises drive force under the constraint that the heeling moment may not exceed the righting moment.

Induced drag is calculated in accordance with lifting line theory [5]:

$$C_{D_i} = kC_L^2 \quad \textbf{(6)}$$

$$k = \frac{1}{\pi A_G} \quad \textbf{(7)}$$

with the geometric aspect ratio, A_G, defined:

$$A_G = \frac{b^2}{S} \quad \textbf{(8)}$$

Marchaj [6] recommends a value of approximately 1.3 for C_{LMax} but this was increased to C_{LMax} = 1.5 for the simulation in light of the developments for modern sails flown from wingmasts which more closely approximate the Moth sail than the tests of Dacron sails flown from masts in [6].

The total aerodynamic drag force is calculated as follows:

$$C_D = C_{D_i} + C_{D_p} \quad \textbf{(9)}$$

$$D = \frac{1}{2}\rho_{air} S_{sail} v_a^2 C_D + D_W \quad \textbf{(10)}$$

and total aerodynamic lift is given by:

$$L = \frac{1}{2}\rho_{air} S_{sail} v_a^2 C_L \quad \textbf{(11)}$$

Lift and drag are then resolved into body axis system:

$$f_y = L\sin(\beta_a) - D\cos(\beta_a) \quad \textbf{(12)}$$

$$f_x = L\cos(\beta_a) + D\sin(\beta_a) \quad \textbf{(13)}$$

and heeling moment is calculated:

$$M = f_x z \quad \textbf{(14)}$$

The value of z in the heeling moment equation is determined from the weighted sum of the perpendicular distances of each contributing heeling force from the centre of effort of the daggerboard.

The centre of effort of the daggerboard is assumed to act at 0.5 times the distance between the free surface and the tip of the daggerboard on account of the rectangular planform of the daggerboard and the end plate effects of both the free surface and the hydrofoil [7].

The centre of effort of the sail is assumed to coincide approximately with the geometric centre of area; at a height of 0.4 times the luff length above the boom.

2.4 Hydrodynamic Force Model

It is assumed that the sailing side force, f_X, is countered entirely by the action of the daggerboard and that the craft adopts whatever lee-way angle necessary to generate this reaction force for the given ship speed. The induced drag on the daggerboard is then calculated accordingly (see 2.4.3)

The VPP searches for the minimum hydrodynamic drag for every combination of ship speed and side force by iterating through the possible foil C_Ls, up to their defined C_{Lmax} values, and evaluating the total hydrodynamic drag in each case.

2.4.1 Flying Condition

The vertical force balance that must be satisfied is:

$$L_1 + L_2 + \Delta_e = W \quad \textbf{(15)}$$

where Δ_e is the effective displacement of the craft and L_1 and L_2 are the lift contributions from the forward and aft lifting foils.

Once the craft becomes fully foil-borne ($\Delta_e = 0$), L_1 and L_2 must satisfy an additional criteria; that there is no net pitching moment.

$$L_1 + L_2 = W \quad \textbf{(16)}$$

$$L_1 x_1 - L_2 x_2 = f_y z^* \quad \textbf{(17)}$$

where z^* is the vertical distance between the centre of effort of drive forces and the centre of effort of resistive forces.

These two simultaneous equations are solved for L_1 and L_2 in order to explicitly define L_1 and L_2 for the fully foil borne case. From this C_{L1} and C_{L2} are determined. This approach is analogous to physical adjustment of the foil trim tabs (which is done automatically by the wand sensor) and relies on the assumption that these balances are achieved solely by the control systems applied to the foils. Implicitly the fore-aft position of the helms-person is assumed to be fixed and constant so that the centre of gravity of the craft does not change position.

The hydrodynamic drag components that are included in the model are the following: Hull residuary and viscous resistance (when $\Delta_e > 0$), daggerboard spray drag (when $\Delta_e = 0$), rudder spray drag, daggerboard induced drag, daggerboard and rudder profile drag, foil 1 and foil 2 induced, profile and wavemaking drag and end-plate profile drag (if end plates are fitted.)

2.4.2 Hull Resistance

Hull residuary resistance is calculated based upon the DELFT regression formula [8] using the effective displacement as the scaling parameter to determine the resistance at a given speed and flying condition.

It is assumed that the residuary resistance varies only as a function of effective displacement, i.e. that the underwater shape of the hull does not change significantly as the effective displacement varies.

The typical hard box shape of a Moth hull means that the shape of the submerged portion of the hull does not change significantly with changes in heave which is a feature that supports this approach.

Hull viscous resistance is calculated using the ITTC '57 skin friction correlation line and a form factor. The scaling factor is the effective wetted surface area which is calculated based on the change in heave necessary to account for the required effective displacement.

2.4.3 Daggerboard Induced Drag

The lift coefficient of the daggerboard is determined by non-dimensionalising the sailing side force, f_X, with respect to the daggerboard wetted area and the ship speed. The wetted area refers to the area of the daggerboard that is below the free-surface. This necessarily reduces when foiling.

In reality the flying height is determined by the control system but in the VPP it is specified by the user. This value is used to determine the span of the daggerboard and rudder remaining below the free surface.

The induced drag of the daggerboard is modelled using the same approach as for the sail (6), but modifying (7), to:

$$k = \frac{1}{2\pi A_G} \quad \textbf{(18)}$$

where a factor of 0.5 accounts for the hull (or free surface when foiling) and lifting foil acting as efficient end plates for the daggerboard [4].

2.4.4 Foil Profile Drag

The calculation of profile drag is the same whether applied to daggerboard, rudder, forward foil, aft foil or end-plates. The skin friction correlation line is used to calculate the skin friction coefficient based on Reynolds number using the mean chord length of the foil as the representative length (3) and (4).

The coefficient of profile drag is calculated as in Hoerner [4, 9] and uses a form factor (Claughton et al. [10]) to allow for the effect of pressure form drag.

$$(1+k) = 1 + 2\frac{t}{c} + 60\left(\frac{t}{c}\right)^4 \quad \textbf{(19)}$$

$$C_{D_p} = 2(1+k)C_f \quad \textbf{(20)}$$

The profile drag is then calculated by dimensionalising with respect to the wetted area, *S*, of the foil and the dynamic head.

$$D_p = C_{D_p}\frac{1}{2}\rho_{water} S v_s^2 \quad \textbf{(21)}$$

The wetted area is modified according to the effective draught of the craft; continuously in the case of the transom hung rudder, and only once fully foil borne in the case of the daggerboard which extends from the underside of the hull.

2.4.5 Foil Induced Drag

The main aim of the VPP is to enable detailed investigation of how variations in foil design affect performance. The drag model for the hydrofoils is therefore more detailed than for the daggerboard, rudder or hull. In particular the induced drag model for the hydrofoils incorporates the effects of taper ratio and end plates (sometimes termed 'winglets') that affect the effective aspect ratio of the foil. The induced drag is calculated as previously:

$$C_{D_i} = kC_L^2 \quad \textbf{(22)}$$

But in this case k is defined using a series of constants to more accurately reflect the changes in effective aspect

ratio of the foil due to the distribution of lift. This is an amalgamation and modification of the results presented in Hoerner [4].

$$k = \frac{1}{\pi AR_g}\kappa_1\left(1+\kappa_2 AR_g\right) \qquad \textbf{(23)}$$

The constant κ_1 reflects the efficiency of the end-plates [4] and is given by:

$$\kappa_1 = \frac{1}{1+2\frac{h}{b}} \qquad \textbf{(24)}$$

According to Hoerner [4] the driver of end-plate efficiency is their area. The end-plates are assumed to be optimally shaped and positioned, and the end-plate is therefore defined solely by its height. The optimal end-plate planform appears to be elliptical with the root chord of the end plate equal to the tip chord of the foil.

The constant κ_2 has the effect of modifying the effective aspect ratio of the foil in accordance with its planform. Thus as the planform approaches an elliptical shape, the effective aspect ratio is maximised. The formula for κ_2 is based on the taper ratio of the foil since it is assumed that, for convenience of manufacture, foils are designed with straight, or near-straight, edges. The data for variation of κ_2 comes from testing carried out by Hoerner [4, 9] on foils with different taper ratios. Regression fitting gives the equation of this relationship in terms of the ratio of tip chord to root chord:

$$\kappa_2 = 0.0624\left(\frac{c_t}{c_r}\right)^4 - 0.1678\left(\frac{c_t}{c_r}\right)^3 + 0.1758\left(\frac{c_t}{c_r}\right)^2 - 0.0725\left(\frac{c_t}{c_r}\right) + 0.0122 \qquad \textbf{(25)}$$

2.4.6 Foil Spray Drag

When foiling both the rudder and daggerboard are surface piercing struts and as a consequence both experience a drag due to the formation of spray. When not 'foiling' the rudder is still a surface piercing strut as it is hung from a gantry some distance behind the transom of the craft. Therefore the hydrodynamic force model always includes the component of spray drag due to the rudder, and does the same for the daggerboard only when fully foil-borne.

This is calculated using a formula due to Chapman [11] that modifies a formula of Hoerner [4] and is based on the thickness – chord ratio.

$$C_{Dspray} = 0.009 + 0.013\left(\frac{t}{c}\right) \qquad \textbf{(26)}$$

$$D_{Spray} = \frac{1}{2}tcv_S^2\rho C_{Dspray} \qquad \textbf{(27)}$$

2.4.7 Foil Wavemaking Resistance

The lifting foil in proximity to the free surface creates a wavemaking effect that carries energy away from the craft in the wave train, and this is manifest as an additional drag component known as wavemaking drag.

Although it is claimed by Martin [12] and Chen [13] that hydrofoil wavemaking resistance is negligible in comparison with the profile and induced drag, it is relatively easy to calculate analytically the form of the wavemaking drag coefficient and foil wavemaking resistance is therefore included in the model for completeness. The coefficient of wavemaking drag can be shown to be related to the wave number, chord length and depth of submersion as follows [14]:

$$C_W = \frac{1}{2}k_0 cC_L^2 e^{-2k_0 h} \qquad \textbf{(28)}$$

with wavenumber $k_0 = \frac{g}{U^2}$ **(29)**

Tip loss drag, associated with the acceleration of flow across the tip of a foil, and junction drag, associated with the interaction of boundary layers at intersecting sections are considered negligible in this model. Added resistance due to waves is also neglected on the basis that waves are associated with wind and in conditions that generate significant waves the craft will almost certainly be fully foil-borne. Modern hydrofoil Moths will typically be fully foil-borne in 5 knots of true wind and above.

3 DISCUSSION OF MODELLING APPROACH AND LIMITATIONS

3.1 Modelling Assumptions

The major simplifications that have been made in the model are:

- The use of the Delft regression formula for hull residuary resistance and the assumption that the change in displacement occurring as the foils generate lift can be modelled simply as a change in heave with negligible impact on waterline beam or length.
- That the position of the centre of effort of sail force is constant (unaffected by twist.)
- Sailing sideforce is generated solely by the daggerboard, and not the hull or rudder.
- No interaction between windage components and that the total windage is equal to the sum of the constituent parts.

Use of the Delft series for residuary resistance is a modelling assumption that is weakest just prior to take-off when the underwater shape of the hull has its greatest distortion from the modelled shape. However, at this speed the effective displacement is very small and the residuary resistance is an almost negligible component of the drag.

The centre of effort of sail force is relatively constant until the craft becomes overpowered at which point increasing amounts of luff tension help the leech of the sail to open and 'twist off' thereby reducing the height of the centre of effort. This effect becomes significant in true wind speeds of approximately 18 knots, but in these conditions boat handling is a more significant factor in speed around the course in comparison to foil design. This wind speed is therefore viewed as an approximate upper limit when considering foil design.

3.2 Model Limitations

Technique aspects of sailing the International Moth that are not captured by the VPP include the tendency to heel the boat to windward when foiling upwind (known colloquially as 'Veal heel'), the fore-aft movement of body weight with changes in speed and apparent wind angle, and techniques such as pumping and 'hotting up' to overcome the drag hump associated with foiling.

3.2.1 Veal heel

Named after the proponent of the technique and multiple foiling Moth world champion, Rohan Veal, 'Veal heel' gives the sailor a greater ability to respond to gusts and lulls, but also has important consequences for the VPP:

- The weight of hull and rig contribute to the righting moment,
- Windward heel causes the lifting foil to share some of the sailing side force, and
- There is a component of sail force acting vertically upwards that contributes to the lifting force from the foils.

The increase in available righting moment due to the positive contribution of the weight of the craft could be up to 10%, based on the lengths and weights recommended for use above and a windward heel angle of 20 degrees. This is probably the most significant effect neglected in the model.

The influence of Veal heel on the re-distribution of sailing side-force between the daggerboard and the lifting hydrofoils has not been investigated but it is likely that the effect will be small for small changes in roll angle: The induced drag of the daggerboard will reduce with increasing windward roll and the induced drag of the hydrofoils will increase. The net change in drag ought to be negligible for small deviations from upright. This aspect of sailing the hydrofoil Moths is a potential area for exploration in future work.

A third important effect of sailing the boat heeled to windward is that the sail force has an upwards component which contributes to the lift from the hydrofoils and thus reduces the induced drag. The complementary effect is that the component of sail force in the drive direction is also reduced, and so it is assumed that for small changes in roll angle the change in net force is negligible.

3.2.2 Fore-aft movement of Ballast

An important aspect of sailing these craft that is not modelled are the fore- and aft- movements made by the sailor to adjust the LCG of the craft in order to achieve the moment balance described in (17). Using the VPP, the position of the LCG of the craft may be varied through a series of cases to examine the effects on performance through the speed range, however it is proposed that this process is incorporated into the VPP automatically so that the optimal position for the sailor (within pre-defined limits) is identified at each time step.

The effect of neglecting variations in the position of the LCG will be most significant at around take-off speed because if not well balanced one foil will still be at max C_L while the other is trimmed back to satisfy the pitch moment condition.

3.2.3 Pumping and 'Hotting up'

There is a drag hump associated with hydrofoil sailing which occurs near take-off speed. At this speed the hull still contributes to the hydrodynamic resistance and is approaching maximum wavemaking resistance, and the foils are at maximum trim to attain maximum lift, which results in large components of induced drag. Once the craft speed increases enough that the craft becomes fully foil-borne, the hull drag disappears and the foils are trimmed back in proportion to the square of the velocity. This reduces the induced drag on the foils, while at the same time the apparent wind speed experienced by the craft increases, giving rise to higher sail forces. Sailors have therefore evolved techniques to help them overcome this drag hump whenever possible and these include pumping and 'footing off' or 'hotting up'.

'Pumping' is a technique of rapidly trimming and releasing the sail in order to generate higher sail force than can be achieved in a steady state.

'Pumping' is not modelled in the VPP but is worth bearing in mind when comparing predicted and measured results, particularly at speeds near to take-off speed.

'Footing off' is the term given to the act of bearing-away from a close hauled course to increase the drive component of sail force. This is used by Moth sailors to overcome the drag hump and they are then able to resume their original windward course ('luff up') once fully foil borne. 'Hotting up' is the analogous process applied when running downwind.

In both cases the craft attains a state that could not have been attained without the course alteration. These techniques are relevant in cases where the craft will foil at some true wind angles but not at others for a given true wind speed. Initially, modelling these techniques is not a primary concern for foil designers, but as the ability of sailors to utilise these techniques increases and the differences between different foil configurations becomes more subtle, these effects will become increasingly important considerations in foil design.

4 IMPLEMENTATION

The VPP algorithm is implemented in Visual Basic and uses Microsoft Excel to supply user-interaction and to output and store results.

Figure 3 shows a flow chart of the computational sequence used in the VPP.

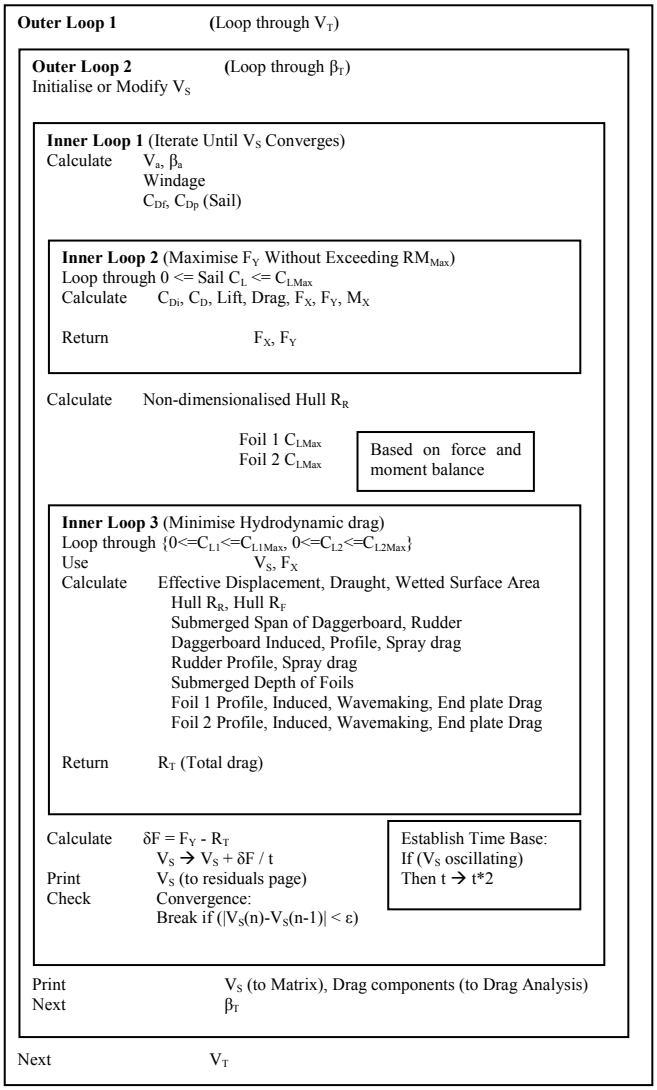

Figure 3 Computational sequence used in VPP.

The time-stepping algorithm uses a variable step size which is reduced if the ship speed exhibits an oscillating behaviour until the ship speed varies monotonically. This reduces computation time as the initial step size is quite large, and allows the ship speed to smoothly attain an asymptotic value that is within convergence limits.

The convergence limit was taken as 0.01% of the ship speed, that is if subsequent iterations of ship speed are within 0.01% of each other (and ship speed is monotonically increasing) then it is deemed to have converged satisfactorily.

In addition to the convergence criterion and the time step there are three constants are used within the program which have a direct bearing on the solution accuracy and these are:

- The step size for incrementing sail C_L
- The step size for incrementing forward foil C_L
- The step size for incrementing aft foil C_L

In each case the sensitivity of the solution to these values was investigated. Starting with a 500 increments for each of the lift coefficients it was found that this number could be reduced to: 250 increments for the sail lift coefficient and 50 increments for each of the foil C_L coefficients without impacting the final solution by more than 0.5%. These values are therefore adopted in order to minimise computational time and the implementation of the model is thought to be accurate to within 1%.

It has not been possible to complete trials of an instrumented hydrofoil Moth in order to verify the predictions of the VPP. Support for the predictions made by the VPP comes from empirical evidence regarding the minimum true wind speed for the craft to become fully foil-borne and the top speed attainable in a range of true wind conditions.

5 RESULTS

5.1 Polar Information

The VPP data is best represented in a polar diagram which shows contour lines of constant true wind strength. Any point on the contour has a distance from the origin which is proportional to the boat speed and an angle from vertical which is equal to the true wind angle. An example is shown in Figure 4 below.

The figure shows that at true wind speeds of 2 and 3 knots the craft cannot attain a foiling state, while at 4 knots of true wind the significant increase in boat speed shows that foiling can be achieved over a range of ‘reaching’ angles. As the wind speed increases the range of angles at which the craft is fully foil-borne increases, as does the speed of the craft. Maximum speed of approximately 11.84 m/s (23 knots) is achieved in 14 knots of true wind, at a true wind angle of 155 degrees.

5.2 Drag Analysis

An analysis can be made of the magnitude of each drag component by taking "snapshots" of the resistance components at a variety of true wind conditions and hence a range of ship speeds. The aim of this feature is to give the designer insight into the effect that parameter selection is having on total drag and target strategies at improving this.

It was necessary to take 'snapshots' of the drag components from the polar information (as opposed to simply prescribing the craft speed and calculating the magnitude of each component) in order to capture the influence of sailing side force on daggerboard induced drag and attain the correct balance of lift forces from the hydrofoils. An example of the drag analysis can be seen in Figure 6.

In order to avoid the contribution due to windage, snapshots were taken at every true wind speed and at apparent wind angles as close to 90 degrees as possible. Nevertheless it can be seen that there is some contribution from windage in some of the 'snapshots'. In Figure 6 this is most noticeable at the highest speed when the apparent wind is marginally aft of the beam and a component of windage acts in the drive direction.

The drag analysis is discussed in more detail in the next section in context of comparison between two different foil set-ups.

5.3 Race analysis

The polar data from the VPP is used to make comparative assessments of craft performance around a race course. In this simulation the race course is assumed to be a windward – leeward course consisting of 2 full laps and a final windward leg to the finish.

It is assumed that boats are sailed at their optimum velocity made good (VMG) towards the next mark. By resolving the polar information into a Cartesian coordinate system, the upwind VMG in a given true wind strength is the maxima of the contour and the downwind VMG is the minima of the contour. The wind is assumed to be steady and the boats spend equal time on each tack as they progress both upwind and downwind.

It is then possible to compare the relative strengths and weaknesses of different foil configurations across the range of true wind conditions both upwind, downwind and in total around the race course.

The 'better' design may be determined using the technique of Oliver *et al.* [15] whereby if the win-margin line crosses the equilibrium point only once, at $v_T = v_T^*$ (so that one yacht would win in true wind conditions of $v_T < v_T^*$, while the other would win if $v_T > v_T^*$), the better design is the design that would win in the expected average wind condition for the regatta. See Figure 8 for an example of a win-loss graph.

It has been found for the hydrofoiling Moths that there are frequently cases in which the win-margin line crosses the equilibrium line twice. In this case the same configuration may prove to be slow in light airs and in heavy airs, but fast in medium conditions. The philosophy of Oliver *et al*. [15] still seems like a sensible one, but requires care in its application.

6 CASE STUDIES

The use of the VPP, drag inspection and race analysis as a design tool is illustrated by some examples. Example 1 examines the effect of changing the span of the forward foil, while keeping all other parameters the same.

6.1 Example 1: Effect of Changing the Span of the Forward Foil

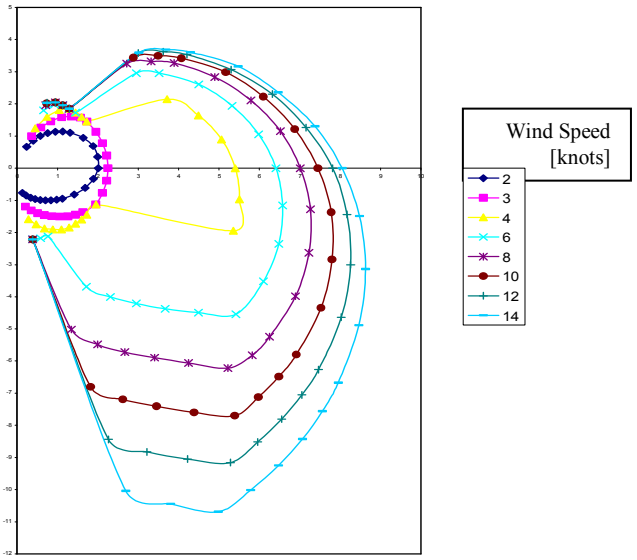

Figure 4 Polar diagram for hydrofoil moth with forward foil of span 1.2m

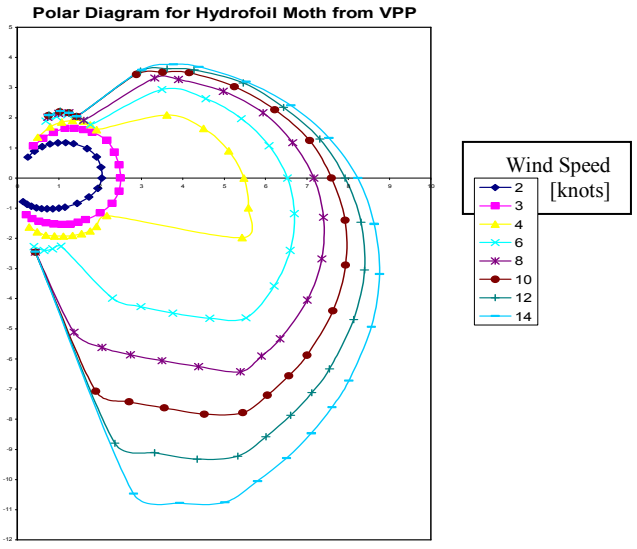

Figure 5 Polar diagram for hydrofoil Moth with forward foil span of 0.85m

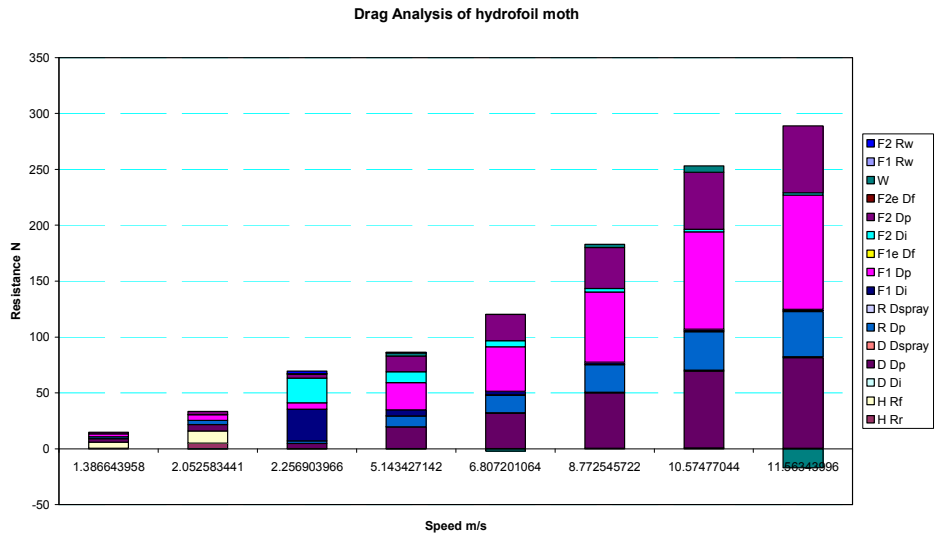

Figure 6 Drag analysis for Moth with forward foil of span 1.2m

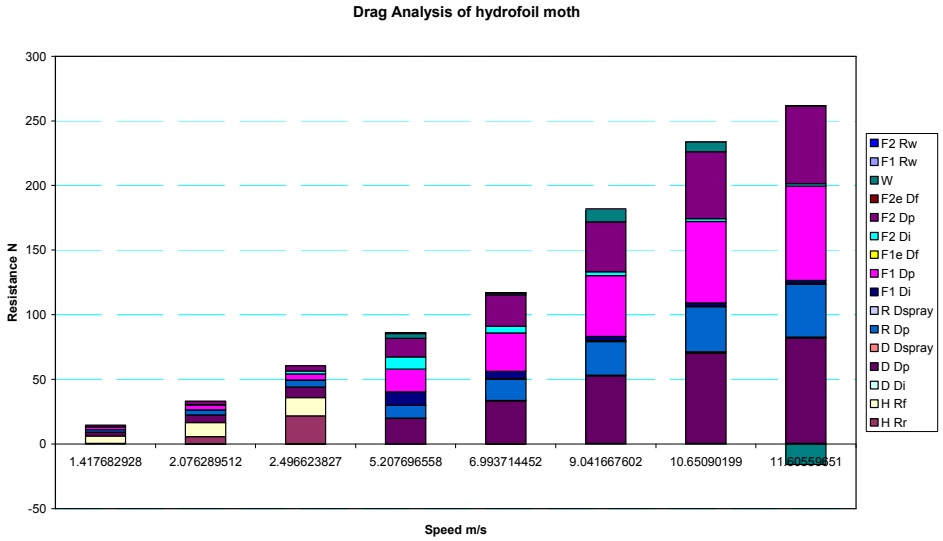

Figure 7 Drag analysis of Moth with forward foil span of 0.85m

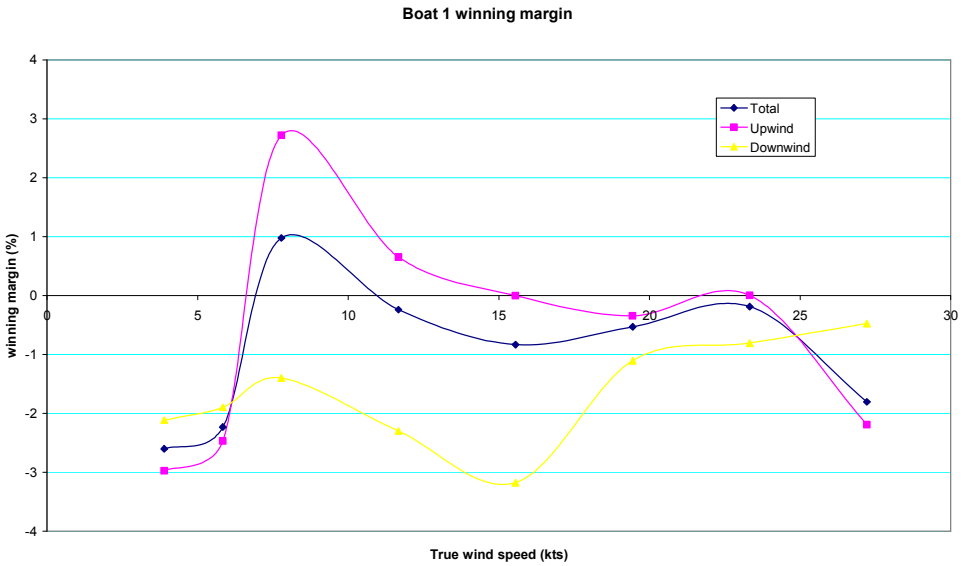

Figure 8 Win-margin graph of Boat 1 (large forward foil) vs. Boat 2 (small forward foil.)

Figure 4 and Figure 5 show the polar diagrams for two identical Moths differing only in the span of the forward foil. In the first instance the Moth has a forward foil span of 1.2m, while in the second the span is reduced to 0.85m. The polar diagrams show that the Moth with the larger forward foil is able to become foil-borne sooner than the other configuration as indicated by the larger regions of high speed at the true wind speed of 4m/s. Other than this, it is hard to make any other observations from the polar diagrams.

Figure 6 and Figure 7 shows the drag analysis as performed at apparent wind angles close to 90 degrees to avoid as much as possible any contribution from windage. Figure 6 is the drag analysis for the Moth with a forward foil span of 1.2m. It can be seen that although the total drag at speeds of just over 2 m/s is reduced due to reduced hull resistance, there is a large increase in drag at the higher speeds due to the large amount of profile drag on foil 1. In addition the requirement to satisfy the condition of zero-net trimming moment when foil borne means that the aft foil is trimmed to its maximum lift coefficient at a relatively low speed, resulting in a high component of induced drag early on.

Upon inspection of the win-margin graph from the race analysis (Figure 8), it can be seen that the configuration using the forward foil with the largest span (Boat 1) under-performs in conditions other than medium-light winds of between 7 and 11 knots true. Boat 2, using the foil with reduced area, performs better over a wider range of conditions, particularly at around 15 knots of true wind speed. Figure 7 shows the drag analysis of this craft, from which it can be seen that the gain around the course is probably due to the reduction in profile drag on the forward foil.

6.2 Example 2: Effects of End-Plates

End-plates reduce induced drag while increasing skin friction. In this example we examine the costs and payoffs of adding end-plates to the standard foil configuration. Boat 1 utilises end plates of height 0.1m on both the fore- and aft- foils, and Boat 2 without end-plates. Both are otherwise identical.

This example begins with an analysis of the win-margin graph from the race-simulation (Figure 9.)

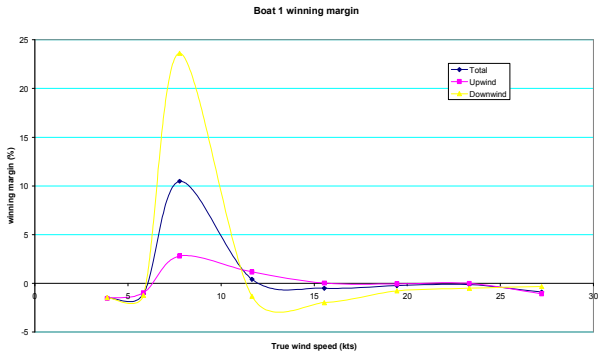

Figure 9 Win-margin graph of Boat 1 (with end plates) vs. Boat 2 (without.)

The race analysis shows that the configuration without end-plates performs very slightly better around the race track in wind speeds of less than about 6 knots and more than about 12 knots.

In the light winds (less than 6 knots), the craft cannot become fully foil borne and so the foils have been feathered in order to remove the components of induced drag. In this case the end-plates have no positive effect on performance but the added surface area increases the total resistance. This can be seen in Figure 10, showing the drag analysis of this craft, which should be compared with Figure 7, the drag analysis of the craft without end-plates.

At the point at which the craft becomes fully foil-borne, the foils are at maximum angle of attack and lift coefficient and the component of induced drag becomes very large (compare Figure 7 with Figure 10 at boat speeds of around 5m/s.) In this case the end-plates play a vital role by increasing the effective aspect ratio of the foil and consequently reducing the induced drag component. The overall effect is a leap in performance such that the craft with end-plates beats the craft without by a margin of around 10% in winds of 8 knots.

As the craft speed progressively increases with increasing true wind speed, the lift coefficients of the foils begin to reduce (the flaps are progressively feathered back towards the zero angle of attack position), and the corresponding component of induced drag reduces. At the same time the skin-friction of the end plates is becoming more significant (Figure 10.) The beneficial effect of the end-plates is therefore reduced and this is reflected in the slight reduction in performance in true wind speeds above 12 knots.

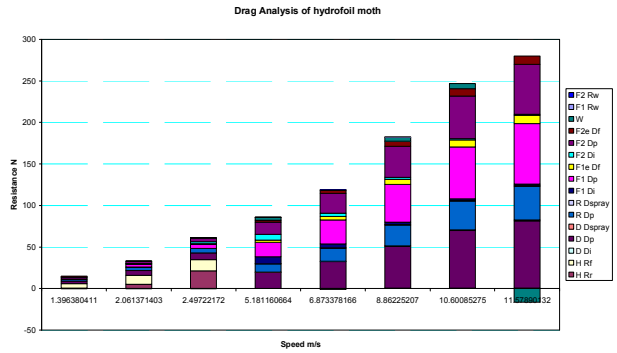

Figure 10 Drag analysis of Moth with end-plates of height 0.1m

6.3 Example 3: Changes to Foil Geometry

In the final example tapered foils are introduced by reducing the chord of the foils at their tips.

In addition the area of the forward foil is reduced by reducing the span and the mean chord (thus maintaining constant aspect ratio.) The motivation for doing this comes from the drag breakdown of the original configuration (Figure 7) which shows that the component of induced drag is small relative to the component of profile drag.

The results of example 2 suggest that end-plates give good performance benefits in some regions without having a particularly detrimental effect elsewhere. The final hypothetical modification is therefore the addition of end plates of height 0.1m on both the fore- and aft-foils to reduce induced drag in the mid-range speeds.

Figure 11 shows the drag analysis of the modified set-up. It can be seen that the induced drag components of both the fore- and aft- foils have dropped significantly. As a result of the decreased foil area the craft does not become fully foil borne until slightly later, exhibiting a clear drag hump at a speed of around 2.7 m/s.

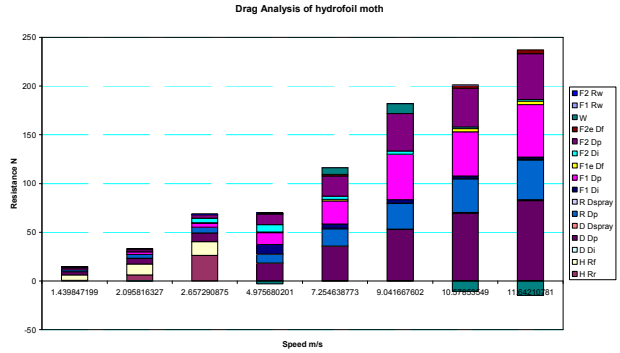

Figure 11 Drag analysis of Moth using modified full force foil set-up

The win-margin graph of the craft using the modified configuration (Boat 1) racing against the existing configuration (Figure 12) shows that the modified configuration performs better across the range of true wind speeds, achieving a winning margin of up to 8% in winds of around 8 knots. The configuration is particularly effective upwind as can be seen from the graph.

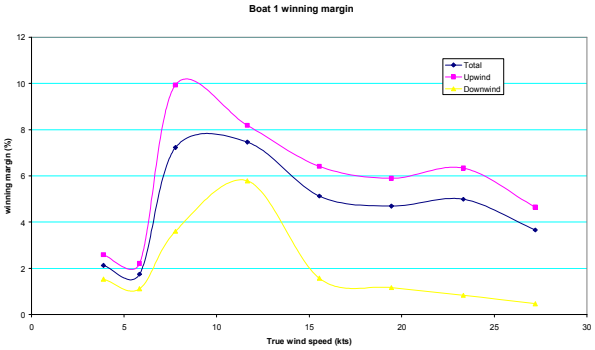

Figure 12 Win-margin graph of Boat 1 (modified foil set-up) vs. Boat 2 (standard set-up.)

7 DISCUSSION

The major target areas for improvements to the program follow from the limitations identified earlier:

- To include the effect of pumping by temporarily 'borrowing' sail force for a short time and seeing if the resulting craft speed is maintainable (apply a small positive disturbance and check to see if a new stable solution occurs.)
- To include 'footing off' and 'hotting up' to get foiling by starting from a foiling condition and moving towards the non-foiling condition while checking for stability in the solution.
- To include fore-aft movement of ballast.
- To include the effects of windward heel.

In addition to these modifications some feedback from the sailors regarding the boat set-up for light winds will be incorporated into future versions of the VPP. In the VPP as used in this paper the foils may be 'feathered' to have minimum C_L if this is the condition that minimises total hydrodynamic resistance. This occurs in very light winds when the craft moves very slowly and the cost (in terms of induced drag) of high C_L is not worth the benefit of the lift generated to raise the hull. In reality the sailors are not able to 'feather' their forward foil in this way and so this behaviour should be constrained in the model.

Recent foil designs have removed the trailing edge flap from the aft foil, opting instead to change the angle of attack of the entire foil, usually by pivoting the rudder in pitch on the rudder gantry. This means that the aft foil is often set prior to sailing in a given wind condition perhaps being adjusted (at most) between upwind and downwind legs of the course. Control is achieved solely through flap adjustment on the forward foil and the fore- and aft- movement of body weight. This is the final behaviour that would be incorporated into an upgraded model.

8 CONCLUSIONS

The case studies give an indication of how the VPP may be used as a tool to aid the designer when making decisions regarding the foil configuration. Further application of the VPP would be to evaluate candidates in optimisation studies using parametric variations or genetic algorithms. The final application of such a tool is as a coaching aid to help the sailor understand in what regions VMG occurs upwind and downwind and to investigate the effects of different fore-aft body positions on foil set-up and performance.

In the two and half years that have elapsed since this research work was initially carried out, International Moths, and in particularly their foils, have evolved a great deal. Each iteration of foil design has increased aspect ratio by increasing span and decreasing chord. Foils have gone from being purely rectangular to first tapered and now entirely elliptical in profile. In the interim gains were made by fitting end-plates but these are again redundant on elliptical profile, high aspect modern foils. It is pleasing that this evolution in foil shapes supports (empirically at least) the indications from the VPP.

9 REFERENCES

[1] Johnston, 'Historical Perspective', 1975.

[2] Chapman, E. J. C. and Chapman G. C., 'The Design and Development of a 4.9m Hydrofoil Catamaran', 2nd Australian Sailing Conference, Hobart, 1999.

[3] Photo: James Boyd www.thedailysail.com Published 27/04/08

[4] Hoerner, S. F., 'Fluid Dynamic Drag', Hoerner, 1965.

[5] Abbot, I. H. and von Doenhoff, A. E., Theory of Wing Sections, Dover Press, 1959.

[6] Marchaj, C. A., 'Aero-hydrodynamics of Sailing', Granade, 1979.

[7] Molland, A. F. and Turnock, S. R., Marine Rudders and Control Surfaces, Butterworth Heinnemann, 2007.

[8] Gerritsma, J., Keuning, J. A. and Onnink, R., 'Geometry, Resistance and Stability of the Delft Systematic Yacht Hull Series', Proceedings of the 5th HISWA Symposium, Amsterdam, 1981.

[9] Hoerner, S. F., 'Fluid Dynamic Lift', Hoerner, 1975.

[10] Claughton, A. R., Shenoi, A. and Wellicome, J. F., 'Sailing Yacht Design – Theory', Addison Wesley Longman, 1998.

[11] Chapman, R. B., 'Spray Drag of Surface Piercing Struts', 1972 AIAA/SNAME/USN Advanced Marine Vehicles Meeting: Annapolis, MD, July 17-19, 1972.

[12] Martin, M. 'The Stability Derivatives of a Hydrofoil Boat', Hydronautics Incorporated, Technical Report 001-10, 1963.

[13] Chen, 'Optimum Wing-Strut Systems for High Speed Operation Near a Free Surface', 1960.

[14] Wellicome, J. F., 'Advanced Marine Vehicles; Hydrofoils', University of Southampton Ship Science Lecture Notes Series, 1998.

[15] Oliver, J. C., Letcher, J. S. J. R. and Salvesen, N., 'Performance Predictions for Stars and Stripes', Transactions of SNAME, NY, 1987.

10 AUTHOR'S BIOGRAPHIES

Matt Findlay is an Engineering Doctorate student at the Fluid Structure Interactions Research Group at the School of Engineering Sciences, University of Southampton. His research interests include yacht aero- and hydrodynamics and engineering applications in high performance sport.

Stephen Turnock is a senior lecturer in the School of Engineering Sciences at the University of Southampton. His research interests are in the area of maritime fluid dynamics and its application to marine energy, underwater vehicles and performance sports engineering.